Effect of ion-implanted Gd on the superconducting properties of thin Nb films*

P. D. Scholten† and W. G. Moulton
Department of Physics, Florida State University, Tallahassee, Florida 32306
(Received 26 July 1976)

Nb films, 400 Å thick, were made by electron-beam evaporation. The four-contact geometry was produced by photoetching, with a 35×76-μm constriction in the center. Gd ions at concentrations between 0.125 and 9.0 at.% were implanted into the Nb films at energies of 50, 100, and 150 keV. The distribution of Gd ions at these energies has been previously measured. It was found that T_c and I_c were strongly dependent on the Gd distribution and that the depression of T_c and I_c decreased with increasing implantation energies corresponding to increased penetration. For each implantation energy, both T_c and I_c showed a rapid decrease for low ($<$ 1-at.%) concentrations of Gd which then leveled off as the concentration increased up to 4 at.%. The fractional depression of I_c was about five times as much as T_c at low Gd concentrations. The T_c data can be qualitatively described by a proximity-effect theory while the depression of I_c was compared to a film-thinning model.

I. INTRODUCTION

A number of studies of the effects of implanted ions on the critical temperature, and other properties of superconducting thin films, have been reported in the literature.[1-6] In the case of nonmagnetic ions, changes in T_c can largely be attributed to radiation damage, whereas for magnetic ions direct Cooper-pair breaking effects play the dominant role, as discussed by Buckel and Heim.[2] In the case of superconducting Nb almost all of the work reported has dealt with implanted impurities that do not possess magnetic moments.[3,4,6] However, Crozat *et al.*[3] have observed magnetic effects for the case of Er implanted into Nb.

We report here the results of our study of the effects of ion-implanted Gd on the superconducting properties of thin Nb films. To our knowledge, the only previously published work on the Nb-Gd system has been by Koch and co-workers.[7,8] Their samples were formed by melting the two elements together. Due to the low solubility of Gd in Nb, these samples consisted of dispersions of Gd globules distributed throughout the Nb bulk. Ion implantation, however, is an effective means of doping a material with an impurity and controlling the distribution regardless of their mutual solubility. In this way we were able to spread the Gd throughout more of the sample and, hence, observe large effects on the critical temperature and critical current.

II. EXPERIMENTAL METHODS

The Nb films were prepared by electron-beam evaporation at a pressure of 5×10^{-6} Torr. The films were evaporated on 3×1-in. glass slides at a rate of about 80 Å/sec with the final thicknesses being approximately 400 Å. The thicknesses were determined by a Sloan quartz-crystal-oscillator digital thickness monitor. The accuracy of the monitor was checked by Rutherford-scattering measurements. The estimated uncertainty in the thickness measurements was $\pm 10\%$. Electron micrographs and x-ray diffraction revealed the films had no crystal structure of dimensions greater than 30 Å.

The desired sample geometry was produced by high-resolution photoetching using Kodak 747 Micro Resist. Each sample employed a four-contact configuration with a narrow geometrical constriction situated at the center of the current path. The dimensions of this bridge were 76 μm long by 35 μm wide; the width of the rest of the current path was 10 mm. Four samples were photoetched on each 3×1-in. slide. The photoetching process was found to be very reliable in producing sharp well-defined bridges, with a width variation of less than 1.0 μm on any given bridge.

An exchange gas system was used for the low-temperature experiments. The slide containing the samples to be measured was bolted to a Cu block with a layer of Apiezon *M* grease applied between the slide and the block to provide good thermal contact. The temperature stability was ± 0.01 °K. Electrical contact was made to the sample by ultrasonically soldering Cu wires to the Nb using In solder.

The low-temperature experiments consisted of measuring the critical current I_c of each bridge as a function of temperature. A pulsed-current system was used to minimize Joule heating effects. The width of the pulses was 70 μsec, and the duty cycle was about 250. Reducing heating effects was important since critical currents were typically around 100 mA at 4.2 °K. (A critical

current of 100 mA corresponds to a J_c of 7×10^6 Å/cm^2.)

The implantation of the Gd was performed with the FSU isotope separator. This machine usually operates with a 50-kV accelerating potential, but by using doubly charged ions 100-keV implantation energies were obtained. Implantations at 150 keV were achieved by using a post accelerator at the end of the separator. The isotope ^{158}Gd was used for the implantation, while ^{160}Gd was monitored to measure the implanted dose. The difference in natural abundance was taken into account in computing the actual implanted dose. The dose figures reported here are accurate to ±15%. Typical Gd doses ranged from 2.5×10^{14} ions/cm^2 for the $\frac{1}{8}$% implants, to 2.1×10^{15} ions/cm^2 for the 1% implants. At such dosage levels, any thinning of the films due to sputtering are calculated to be within the ±10% uncertainty in the thickness. No thinning was observed to within the ±10% uncertainty in the measurements of thickness determined by Rutherford scattering and optical density.

We have previously reported[9] a series of experiments designed to determine the distribution of Gd implanted into Nb. The distribution profiles, shown in Fig. 1, were obtained through nuclear backscattering measurements and a computerized deconvolution procedure. Owing to subsequent corrections, the depth scale in Fig. 1 has been changed very slightly from that appearing in the previous publication.[9]

For each slide run, only the center two bridges were implanted; the other two were used as controls to monitor any aging effects on the superconducting properties. It was generally found for

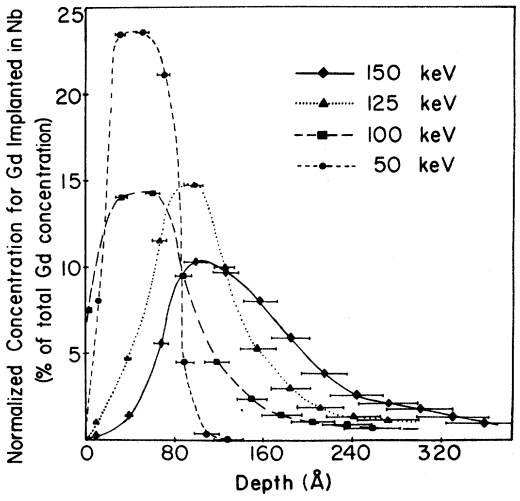

FIG. 1. Distributions of Gd implanted into Nb for energies between 50 and 150 keV.

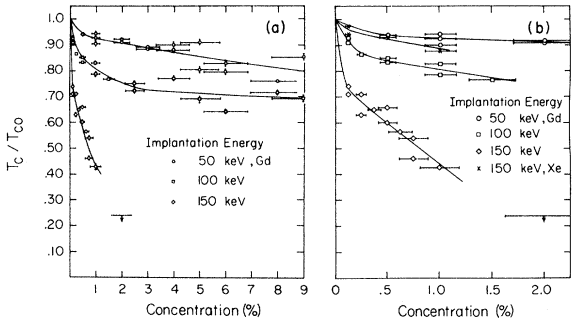

FIG. 2. Reduced critical temperature as a function of Gd concentration. Here, T_c is the critical temperature of the sample after implantation and T_{c0} is the critical temperature before implantation (typically 6.5°K). In (b) the low-concentration data are repeated with the low-concentration scale expanded. The lines drawn through the data are only included for clarity and do not represent any theory or best fit to the data.

a control sample that the measured critical currents at all temperatures decreased a very small amount, typically about 1 mA, with age. This aging period (time between runs) varied from about 10 days to more than 50 days. The change in T_c was no more than 0.02 °K. The effects of aging on the critical temperature and critical current data shown in Figs. 2 and 3 were incorporated into the experimental uncertainty estimates, ±0.01, shown in the figures.

III. RESULTS

The effect on the critical temperatures of the Nb films due to the implanted Gd is shown in Fig. 2. The critical temperature of a film was determined by linearly extrapolating the I_c vs T curve to $I_c = 0$. Values of T_c were around 6.5 °K for

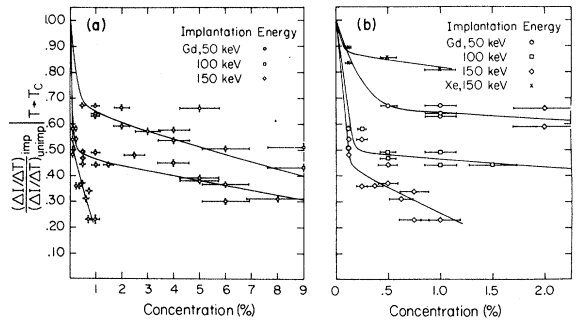

FIG. 3. Ratio of the slopes, as $T\to T_c$, of the I_c- vs $-T$ curves (implanted bridge divided by unimplanted bridge) as a function of Gd concentration. The low-concentration data are repeated in (b) with the low-concentration scale expanded. The lines drawn through the data are only included for clarity and do not represent any theory or best fit to the data.

the unimplanted films, typical of highly disordered films containing some oxygen. This point is discussed later. Several measurements of T_c were made using a dc method at a current of 1.00 μA, and the results of these measurements gave values of T_c well within experimental error of the extrapolated I_c-vs-T curves. The width of the transition was about 0.2 °K in the unimplanted films. The implanted dose figures were computed on the basis of a homogeneous Gd distribution, using the entire film thickness. Although the actual distributions are clearly not homogeneous, the given dosage figures are nonetheless a useful measure of the amount of impurity in each film. Figure 2 also shows an enlargement of the low-concentration region. Whereas the 50-keV data show a smooth and only slight drop in T_c, the 100 keV, and especially the 150-keV implants, exhibit a sharp initial drop in T_c followed by a trend toward saturation.

The reduction in the critical current is shown in Fig. 3. It can be seen from the figure that the fractional depression of I_c is significantly more than that of T_c in every case. As a measure of the depression of the critical current, we have used the ratio of the slopes as $T \to T_c$ of the I_c-vs-T graphs of the implanted and unimplanted samples. The relationship between I_c and T was quite linear in the measured region (generally, 4.2 °K up to T_c) with a slope of about -40 mA/°K. Since we were interested in examining the depression of I_c as a function of impurity concentration, it was necessary to attempt to remove the influence of T from the relationship between I_c and the impurity concentration. Since I_c was highly dependent upon T, any decrease in T_c of a sample brought about by impurity effects would automatically result in lower measured I_c values at a particular T. We felt that the general results of a theory for critical fields should be applicable to critical currents since the intrinsic critical current of a superconductor is directly proportional to the thermodynamic critical field which, in turn, is directly proportional to H_{c2}. The particular equation used, derived for the case of a dirty type-II superconductor for $|T - T_c| \ll T_c$ was[10]

$$H_{c2}^{*} = \frac{4ck_B T_c}{3v_F el}\left(1 - \frac{T}{T_c}\right) \times \left[1 - \left(1 - \frac{T}{T_c}\right)\left(\frac{1}{2} - \frac{28\zeta(3)}{\pi^4}\,(1-\alpha^2)\right)\right],$$

where

$$H_{c2}^{*} = (1/H_{c2}^2 + 1/H_p^2)^{-1/2},$$

H_p is the critical field in the paramagnetic limit,

$$\alpha = \sqrt{2}\,[H_{c2}(0)]/[H_p(0)],$$

and l = electronic mean free path. For materials like Nb which have values of κ that are not much greater than 1, H_{c2} will be much smaller than H_p. Therefore, we replaced H_{c2}^{*} with H_{c2}.

The slope of the curve defined by this equation is, in the limit of $|T - T_c| \ll T_c$,

$$\frac{dH_{c2}}{dT} = \frac{-4k_B C}{3v_F el}.$$

Thus, the slope of the critical-field curve, at $T = T_c$, is temperature independent. We assume that this will also be the case for the critical-current curve. Temperature effects on the value of l were believed to be negligible in this narrow temperature range. Since the slope of the I_c-vs-T curve, as $T \to T_c$, is not dependent upon T, it should be a valid measure of the effect of the Gd impurity concentration on the critical current.

To determine how much of the depression of T_c is due to the magnetic nature of the Gd, the effects of 150-keV Xe implants were also studied. The results of these experiments are presented in Figs. 2(b) and 3(b). Since they are less massive than the Gd, the Xe ions have a mean range about 10% greater than that of the Gd according to the Lindhard, Scharff, and Schiott (LSS) theory[11] (although the mean range of Gd implanted into Nb does not follow the LSS theory,[9] we feel that using LSS to estimate the range difference between Gd and Xe is an adequate first-order approximation). The standard deviation of the Xe distribution is also about 10% larger than that of Gd. Since the Xe ions are definitely nonmagnetic in the Nb, we attribute all of the difference in the T_c and I_c depressions between the Xe and Gd to be due to the magnetic nature of the Gd. Examples of nonmagnetic effects due to the bombardment of the films by heavy ions include radiation damage and possible redistribution of the oxygen present in our films. We would expect damage effects to be small in these films, since they are highly amorphous.

Studies of the change in T_c of various superconductors due to radiation damage produced by the implantation of heavy ions have been reported elsewhere.[1-4] Buckel and Heim[2] have studied, along with other combinations, the ion implanted system of Pb-Mn in comparison with that of Pb-Zn. They used several implantation energies in producing each system in an effort to create as homogeneous an impurity distribution as possible. Their data show that radiation-damage effects are only comparable to magnetic effects at low concentrations (< 50 ppm in their system). As the ion concentration increases, the damage effects saturate while the magnetic effects continue to depress T_c. In the Nb-Gd system it can be seen

that magnetic effects clearly dominate nonmagnetic effects although in this case both the magnetic and nonmagnetic effects tend to saturate. These saturation effects are believed to be related to the impurity distribution. This point will be discussed later.

Several different ions have been implanted into Nb by Crozat *et al.*[3] Their results show also that magnetic ions produce a greater suppression of T_c than nonmagnetic ions. However, their damage effects are generally greater than ours for equal doses (effect of 130-keV Nb vs 150-keV Xe). This is probably a result of their Nb films having a greater degree of order than ours. We feel that Meyer *et al.*[4] observed much greater T_c depressions in their Nb-Ar systems for the same reason.

Since our Nb films were stored in open air, we expect a significant amount of oxygen to be present in the upper 30 Å of the film. There will also be oxygen present deeper in the film as a result of the pressure (5×10^{-6} Torr) during film growth. It is possible that some of the incoming Xe or Gd ions could have collided with oxygen atoms, particularly in the surface layer, and transferred enough energy for the oxygen to have penetrated deeper into the Nb. Enhanced quantities of O_2 deeper in the film would serve to depress T_c. Desorbo[12] has shown that O_2 depresses the T_c of Nb at a rate of about 0.9 °K per at.%.

IV. ANALYSIS

It is clear that in analyzing the effect of the implanted Gd on T_c, one must involve the impurity distribution in some manner. From looking at the distribution profiles one could consider an implanted film as being made up of two layers—an upper layer heavily doped with impurity and a lower layer only lightly doped. The heavily doped upper layer would most likely be in the normal state due to the pair-breaking effect of the magnetic Gd while the lower layer would still be superconducting. Such a picture of a normal layer superimposed on a superconducting film suggests that the depression of the critical temperature might be explained by a proximity effect. The proximity-effect theory, to our knowledge, offers no explicit predictions as to the effect of a normal layer on the critical current of a superconducting layer directly beneath it. However, the model for this system as a two-layer configuration implies that for the critical-current behavior a simple film-thinning calculation should apply.

The proximity effect for superconducting films has been the subject of many investigations.[13-17] This previous work has established that the presence of the normal layer is very significant in determining the critical temperature of the superconducting-film–normal-film sandwich.

To predict the change in T_c using the proximity-effect model, we used the theory as developed by Werthamer.[15,16] The equations which describe the problem are

$$\ln(T_{cs}/T_{cp}) = \psi(\tfrac{1}{2}\,\xi_s^2 k_s^2 + \tfrac{1}{2}) - \psi(\tfrac{1}{2})\,, \tag{1}$$

$$\ln(T_{cn}/T_{cp}) = \psi(-\tfrac{1}{2}\,\xi_n^2 k_n^2 + \tfrac{1}{2}) - \psi(\tfrac{1}{2})\,, \tag{2}$$

$$N_s \xi_s^2 k_s \tan(k_s d_s) = N_n \xi_n^2 k_n \tanh(k_n d_n)\,, \tag{3}$$

where

$$\xi_{s,n}^2 = \pi\hbar k_B / 6e^2 T_{cp} \rho_{s,n} \gamma_{s,n}\,,$$

$\psi(x)$ is the digamma function of x, ρ is the low-temperature resistivity, γ is the electronic specific-heat coefficient, N is the density of states at Fermi surface, d_s is the thickness of superconducting layer, d_n is the thickness of normal layer, T_{cs} is the critical temperature of superconducting layer, T_{cn} is the critical temperature of normal layer (initially assumed to be small but finite), and T_{cp} is the critical temperature of ideal-proximity sandwich.

In order to describe our system as consisting of two layers it was necessary to determine where the boundary between the layers should be. An arbitrary value of Gd concentration in a 10-Å-thick layer of 0.5% or greater was assumed to destroy the superconductivity. This depth was taken to be the boundary depth. For the purpose of determining quantities to be used in the theory, we set d_n equal to this boundary depth, and hence, d_s is the total film thickness minus d_n.

The low-temperature resistance of each sample was measured both before and after implantation. From the known geometry of the sample and the unimplanted resistance, ρ_s was calculated. The resistivity of the film after implantation was determined similarly. Once the thicknesses of the two layers were determined for a film, the resistances of d_n and d_s in the bridge were calculated by assuming that the resistance of these layers could be summed as in a parallel network. From the resistance of d_n, ρ_n was calculated.

The γ for pure Nb was used for γ_s. The value for γ_n had to be estimated. To determine roughly the decrease in N due to the Gd impurity, and hence γ, γ_N was calculated from the free-electron model. While the actual values of N and γ probably differ from the bulk values, it was felt that the bulk values would be adequate for a qualitative model. The results of the calculation give an estimate of $\gamma_N = 0.9\,\gamma_s$. Since γ and N are directly proportional to each other in this model, the constant of proportionality cancels in Eq. (3). Thus, N_s and N_n were re-

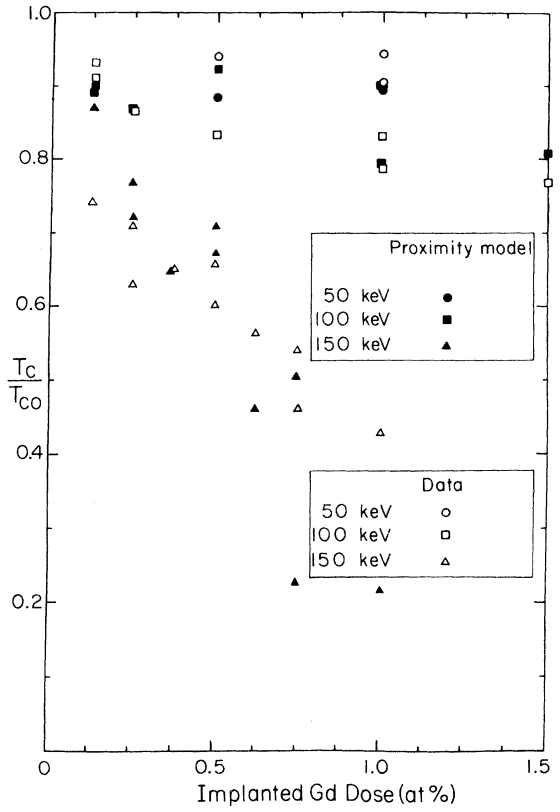

FIG. 4. Comparison between the predictions of the proximity-effect theory and the data for the relationship of reduced critical temperature as a function of Gd concentration. The theoretical results (solid symbols) were computed for each film sample individually and are presented, therefore, as a series of points. For the theoretical points the quantity T_c refers to T_{cp}, defined in the text. For the experimental points (open symbols) T_c refers to the critical temperature after implantation. T_{c0} in both cases is the temperature of the film sample before implantation.

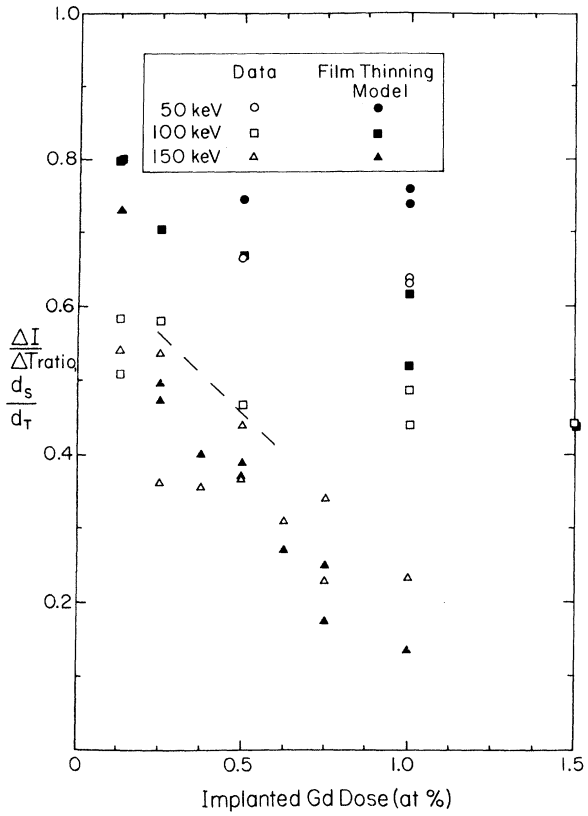

FIG. 5. Comparison between the predictions of the film-thinning model and the data for the relationship of the critical current as a function of Gd concentration. Two different quantities are plotted on the vertical axis. The $\Delta I/\Delta T$ ratio is used for the data points (open symbols) and is the same quantity used in Fig. 3. The quantity d_s/d_T, thickness of superconducting layer divided by total film thickness, is used for the theoretical points (solid symbols). The dashed line is only to clearly separate the 100- keV points from the 150- keV points for concentrations between 0.25 and 0.5 at %.

placed with γ_s and γ_N.

The quantity T_{cs} in Eq. (1) was set equal to the measured critical temperature of the unimplanted sample. In this approximation the effect of the Gd in the tail of the distribution is ignored. In Eq. (2) we set $T_{cn}=0$ since Hauser *et al.*[15] have stated that the theory is rather insensitive to this quantity, and we expected it to be small in any case.

The results of the model calculations are shown in Fig. 4 along with experimental data. The model calculations were made on a sample by sample basis with the quantities d_n, d_s, ρ_n, ρ_s, and T_{cs} having been determined for each individual sample. There appears to be qualitative agreement which suggests that a proximity effect is likely to be present in our implanted samples. One must be careful not to read too much into these results. Besides not having two distinct layers, the distribution profiles have a 10% uncertainty in depth and the unimplanted doses are about 15% uncertain. Furthermore, some of the parameters, particularly the boundary depth, were chosen in an arbitrary manner.

We now consider what predictions could be made for the depression of the critical currents on the basis of a simple two-layer model. In this model it seemed reasonable that the current would flow only in the superconducting layer d_s and therefore, the critical current I_c measured was actually the I_c of d_s. Note that although this film-thinning model for critical currents is not part of the proximity effect model, we used the same values of d_s in both for consistency. Taking the critical

current density of d_s to be equal to that of the unimplanted film, it would be expected then that I_c would be directly proportional to d_s.

Figure 5 shows a comparison of this film thinning model with the experimental data. The quantity d_s/d_t (d_t is the total film thickness) was used because it is equal to unity for a 0% dose as in the $\Delta I/\Delta T$ ratio. The results of this calculation agree qualitatively with the data. To produce a better quantitative agreement, smaller values of d_s would have to be chosen for nearly every sample. This may indicate that the magnetic impurities present in d_s are also active in lowering I_c.

V. CONCLUSIONS

The results of these experiments allow the following conclusions to be reached:

(i) The effect of T_c and I_c due to the implanted Gd is very much dependent upon the impurity distribution.

(ii) The magnetic effects of the Gd at these dose levels are more significant than nonmagnetic effects such as radiation damage.

(iii) The critical current of an implanted film is depressed much more than the critical temperature.

(iv) The depression of T_c of this implanted system may be at least qualitatively described by a proximity effect model, and the depression of the I_c is in qualitative agreement with a simple film-thinning model.

ACKNOWLEDGMENTS

We would like to thank R. Leonard, L. Peirce, B. Engle, and D. Sanford for their expert technical assistance. We especially appreciate the many useful discussions with R. C. Morris, and his critical reading of the manuscript, and the suggestions of M. Strongin regarding this work.

---

*Research supported by AFOSR, Air Force System Command, USAF, under Grant No. AFOSR-75-2769.

†Present address: Dept. of Physics, Texas A&M University, College Station, Tex. 77843.

[1]W. Buckel, M. Dietrich, G. Heim, and J. Kessler, Z. Phys. 245, 283 (1971).

[2]W. Buckel and G. Heim, in *Applications of Ion Beams to Metals*, edited by S. T. Picraux, J. G. EerNisse, and S. L. Vook (Plenum, New York, 1974), p. 35.

[3]P. Crozat, R. Adde, J. Chaumont, H. Bernès Bernas, and D. Zenatti, p. 27.

[4]O. Meyer, H. Mann, and E. Phrilingos, in Ref. 2, p. 15.

[5]G. Heim and E. Kay, J. Appl. Phys. 46, 4006 (1975).

[6]C. H. Arrington and B. S. Denver, Appl. Phys. Lett. 26, 204 (1975).

[7]C. C. Koch and G. R. Love, J. Appl. Phys. 40, 3582 (1969).

[8]C. C. Koch and D. M. Kroeger, J. Less Common Metals 40, 29 (1975).

[9]P. D. Scholten, M. R. Skokan, K. W. Kemper, and W. G. Moulton, Phys. Rev. B 13, 42 (1976).

[10]D. Saint-James, E. J. Thomas, and G. Sarma, *Type II Superconductivity* (Pergamon, Oxford, 1969), p. 171.

[11]J. Linhard, M. Scharff, and H. E. Schiott, Mat. Fys. Medd. Dan. Vid. Selsk. 33, 1 (1963).

[12]W. DeSorbo, Phys. Rev. 132, 107 (1963).

[13]P. Hilsch, Z. Phys. 167, 511 (1962).

[14]H. Tsuya, J. Phys. Soc. Jpn. 20, 1734 (1965).

[15]J. J. Hauser, H. C. Theurer, and N. R. Werthamer, Phys. Rev. 142, 118 (1965).

[16]N. R. Werthamer, Phys. Rev. 132, 2440 (1963).

[17]G. Gladstone, M. A. Jensen, and J. R. Schrieffer, in *Superconductivity*, edited by R. D. Parks (Dekker, New York, 1969), Vol. 2, p. 734.